Electronic Supplementary Information for Dalton Transactions

Supplementary Information

Structure-Related Frustrated Magnetism of Nanosized Polyoxometalates: Aesthetics and Properties in Harmony

Paul Kögerler,[1,*] Boris Tsukerblat,[2] and Achim Müller[3]

(1) Institut für Anorganische Chemie, RWTH Aachen, D-52074 Aachen, Germany and Institut für Festkörperforschung, Forschungszentrum Jülich, D-52425 Jülich, Germany;
E-mail: paul.koegerler@ac.rwth-aachen.de
(2) Department of Chemistry, Ben-Gurion University of the Negev, 84105 Beer-Sheva, Israel
(3) Fakultät für Chemie, Universität Bielefeld, D-33501 Bielefeld, Germany

Principles of spin frustration

The concept of spin frustration has been introduced by Toulouse[81] to describe the phenomenon of spin-glass behavior. Spin frustration implies that in a classical spin representation a set of competing spin-spin interactions can not be completely 'saturated', i.e. no collinear, antiparallel orientation of all spin vectors is achieved. An equilateral spin triangle with antiferromagnetic exchange coupling forcing the spins to align antiparallel represents a widely used example. This kind of spin array is typical for a variety of polynuclear coordination compounds with interesting and unusual properties[39,40,82,83] and low dimensional lattices. Interest in spin frustration is also driven by its potential to explain conduction mechanisms in high-T_C cuprate superconductors where it was proposed that the resonating valence bond state may explain the scatterless hole transport in doped rare-earth cuprates.[84] The quantum spin liquid phase responsible for resonating valence bond state can be found in low-dimensional low-spin frustrated systems. Many theoretical investigations on this issue are focused on s =1/2 Kagomé antiferromagnets based on triangular lattices.[83-91]

We will consider spin-frustration in a triangular unit composed of antiferromagnetically coupled s = 1/2 spins in more detail in order to reveal some physical consequences of spin frustration. Due to the trigonal geometry of the system antiparallel alignment is possible within any selected pair (Fig. S1), whereas the third spin (encircled in black) cannot pair to minimize the energy of the exchange with spins 1 and 2 simultaneously, and in this sense proves to be frustrated. As this classical spin picture cannot provide meaningful physical information, the problem requires a quantum mechanical approach.

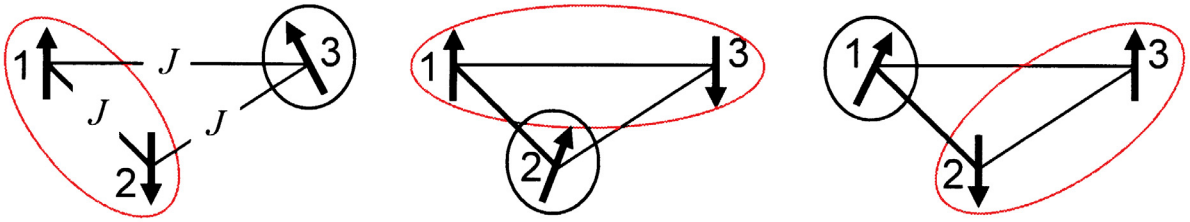

Fig. S1 Scheme of classical spin frustration in a triangular unit.

The energy pattern involves two energy levels $\varepsilon_0(S)$ with S = 1/2 and S = 3/2 that are separated by an energy gap of $3|J|$. It is essential that they do depend upon the full spin S and are independent of S_{12} where $S_{12} = S_1 + S_2$ represents the intermediate spin in the three-spin coupling scheme (for an s = 1/2 triangle, S_{12} = 0 and 1). This leads to the two-fold 'accidental' degeneracy of two S = 1/2 doublets (four-fold degeneracy including two spin projection for each S = 1/2), a seeming contradiction to Kramers theorem. One can see that spin frustration in the ground state is closely related to the degeneracy of the ground spin doublet states $(S_{12})S$ = (0)1/2, (1)1/2 with respect to two allowed values of the intermediate spin S_{12} in the three-spin coupling scheme. For our purposes this model also applies to more complicated systems such as $\{V_{15}As_6\}$ in which the energetically lowest S = 1/2 and 3/2 states resulting from a (weakly coupled) central spin triangle (which determine the low-temperature magnetic properties of this system) are energetically well separated from the remaining levels of the magnetic excitation spectrum. This can be seen from a first calculation of the full set of the spin levels of the $\{V_{15}As_6\}$ cluster based on the irreducible tensor operator method[41,81] and estimated exchange parameters (Fig. S2).[14,36]

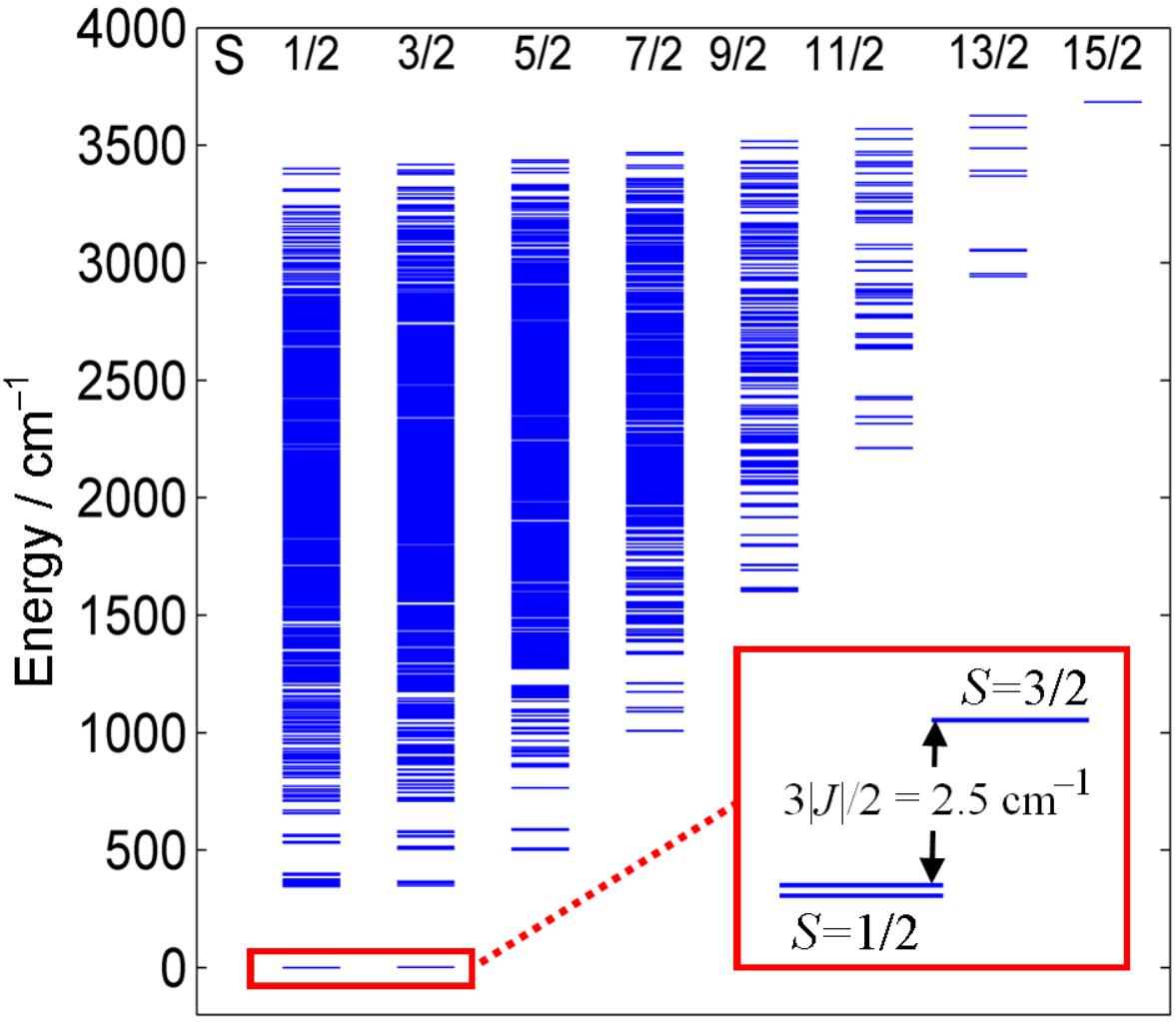

Fig. S2 Magnetic excitation spectrum for $\{V_{15}As_6\}$ showing all eigenvalues grouped by their total spin quantum number S and highlighting the energy separation between the lowest S = 1/2, S = 3/2 levels (relative energies of which are illustrated in the inset) of the spin-frustrated central V_3 triangle and the other spin levels.

Initially, spin frustration appears as a terminological problem implying only that the classical "up-down" picture is inappropriate for the description of this situation. Especially relevant for the concept of spin frustration is the analysis of the physical phenomena, e.g. the excessive degeneracy mentioned above. The analysis of the HDVV Hamiltonian[39,40] revealed that the "degeneracy doubling" with respect to the intermediate spin within the spin coupling scheme in the ground manifold $(S_{12})S$ = (0)1/2, (1)1/2 is associated with the exact orbital degeneracy in the multi-electron triangular system so that the ground term is represented by the orbital doublet ^2E of the trigonal point group, whereas the excited one is the orbital singlet $^4A_2$. A quantum mechanical study of the more complicated systems (for example, triangular clusters with half-integer spins $s \geq 1/2$) shows that spin frustration is inherently related to the orbital

degeneracy of the spin multiplets. This immediately leads to the conclusion that the ground state is unstable with respect to both anisotropic spin-spin interactions and spin-vibrational Jahn-Teller coupling; the first kind of such interaction is represented by the antisymmetric (AS) exchange introduced by Dzyaloshinsky[37] and Moriya[38] as an origin of spin canting. Whereas the isotropic exchange aligns spins parallel or antiparallel (Fig. S3a), the AS exchange (expressed as the vector product $[\boldsymbol{S}_1 \times \boldsymbol{S}_2]$) itself tends to align spins in perpendicular directions (Fig. S3b). Since isotropic exchange usually constitutes the dominating interaction, the competition of isotropic and AS exchange usually results in a relatively small canting angle of the two spins in a dimeric unit, in particular, for $S_1 = S_2 = 1/2$ the canting angle is defined as $\alpha = D/2|J|$, see Fig. S3c for an antiferromagnetic dimer. From the quantum-mechanical point of view AS exchange leads to a small mixing of different spin multiplets ($S = 1$ and $S = 0$ in an $S_i = 1/2$ dimer) giving rise to a zero-field splitting (proportional to D^2/J) and magnetic anisotropy of the spin triplet.

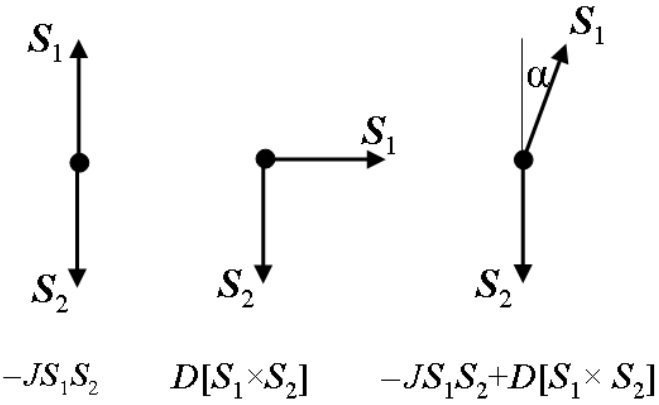

Fig. S3 Classical spin alignment in a spin dimer caused by antiferromagnetic isotropic exchange (a), AS exchange (b), and combined isotropic and AS exchange interactions (c).

An important feature of the spin frustrated triangular system is that its ground state is orbitally degenerate (an orbital doublet ^2E) and therefore unstable with respect to first-order (but not second-order) splitting of the orbitally degenerate multiplets by AS exchange. In a classical interpretation this frustrated spin system is 'soft' in the sense that the AS exchange is not competitive (in contrast to the situation in a dimer) to the isotropic exchange (forming an isolated degenerate multiplet) and gives rise to a specific triangular spin alignment structure defined by a 120° relative angle of neighboring spins rather than to a small canting angle. There are two possibilities for spin configurations depending on the so-called vector of chirality $\boldsymbol{K}$ defined as

$$\boldsymbol{K} = \frac{2}{3\sqrt{3}}([\boldsymbol{S}_1 \times \boldsymbol{S}_2] + [\boldsymbol{S}_2 \times \boldsymbol{S}_3] + [\boldsymbol{S}_3 \times \boldsymbol{S}_1]). \qquad \text{(eq. 5)}$$

For the coplanar arrangement, this vector is parallel to the *c* axis with an amplitude of +1 or –1. By convention the chirality is +1 when the spins rotate clockwise by 120° as one traverses around a triangular plaquette clockwise,[88] in this case according to the definition of the vector product $\boldsymbol{K}$ equals +1 (Fig. S4a). For the spin arrangement depicted in Fig. S4b, $\boldsymbol{K}$ equals –1. Fig. S5 shows two possible spins arrangements in a Kagomé lattice (Fig. 2): (a) a spin arrangement with uniform positive vector chirality and (b) an alternative spin arrangement with staggered vector chirality.

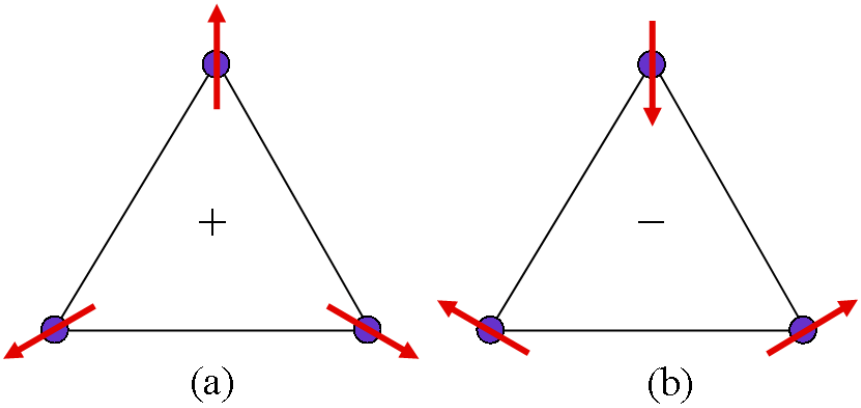

Fig. S4 Triangular spin structures illustrating chirality of +1 (a) and –1 (b).

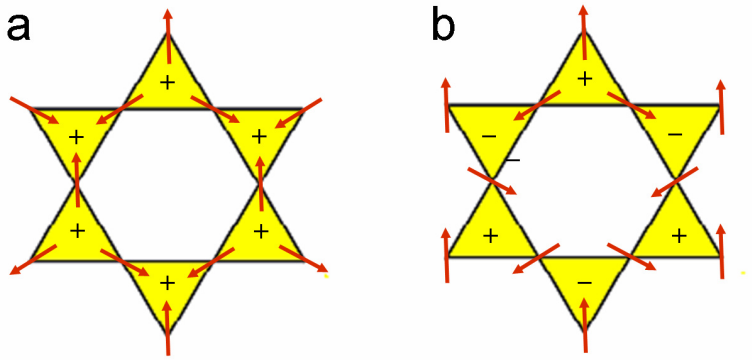

Fig. S5 Two possible spins arrangements in a Kagomé lattice: (a) spin arrangement with uniform positive vector chirality (indicated by + within each triangle) and (b) alternative spin arrangement with staggered vector chirality.

It was recently demonstrated that certain classes of Mott insulators (which usually are geometrically frustrated) exhibit unexpected charge effects: for certain spin textures, spontaneous circular electric currents or non-uniform charge distribution exist in the ground

state of Mott insulators.[92] This is a direct consequence of the so far mentioned orbital degeneracy of the ground state in the spin-frustrated triangles. More complex systems (e.g. a spin cuboctahedron and icosidodecahedron) as well as new interesting manifestations of spin frustration are considered in ref. 93.

Spin-frustrated triangular systems in the doubly degenerate ground state are structurally unstable.[94] In fact, the Jahn-Teller (JT) theorem states that a fully symmetric (trigonal) configuration is unstable due to interaction of the system with double degenerate (*E* type in a trigonal symmetry) vibrational modes (Fig. S6) that decrease the trigonal symmetry of the system, the so-called JT $E \otimes e$ problem.[94] The interaction of the spin system with the vibrational degrees of freedom appears due to the modulation of the (mainly) isotropic exchange interactions by displacement of the sites; the parameter of this interaction υ (proportional to the derivative of the exchange parameter over displacement) is explicitly defined in ref. 95. If the AS exchange is neglected the adiabatic surface of the system represents a "sombrero" in the space of the *E* type vibrations (Fig. S7). Within a semiclassical context this means that the system runs over distorted geometrical configurations for which the orbital degeneracy is removed (Fig. S8).

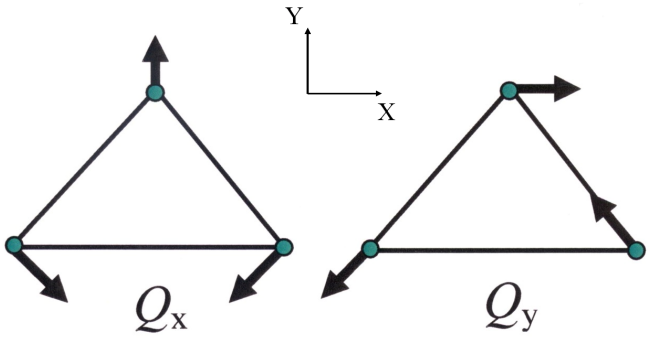

Fig. S6 Displacement of the magnetic sites in double-degenerate (*E*) vibration of a triangular cluster.

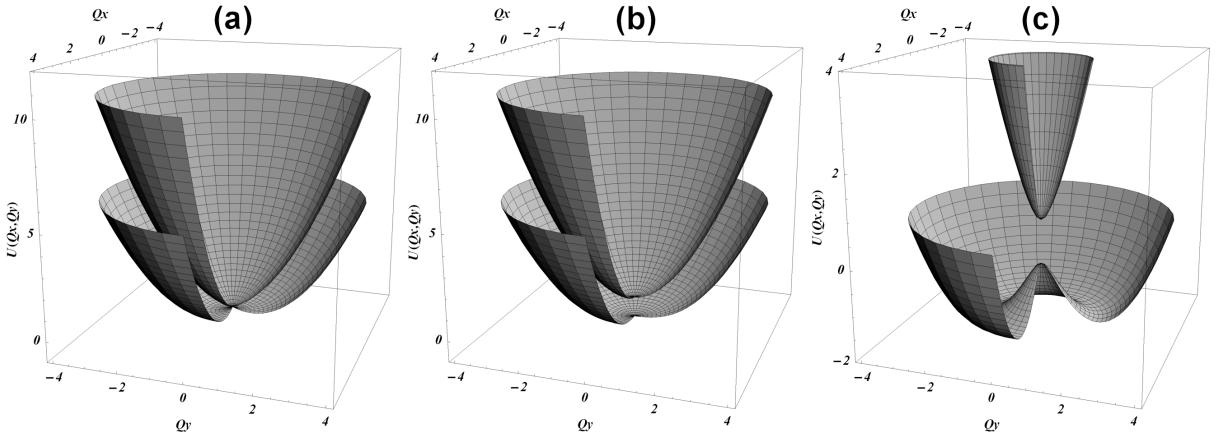

Fig. S7 Adiabatic potentials for the ground state of a triangular exchange system in the space of the double degenerate vibrations: (a) $\delta = 0$, $\upsilon = 2.0$; (b) weak vibronic interaction and/or strong AS exchange ($\delta = \upsilon = 1.0$); (c) weak AS exchange and/or strong vibronic interaction ($\delta = 1.0$, $\upsilon = 3.0$).

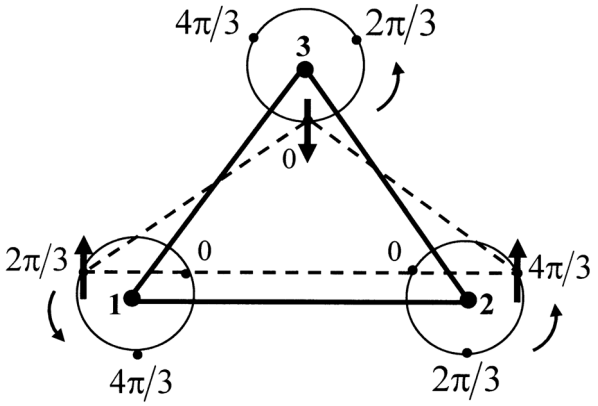

Fig. S8 Rotation of the distorted configurations (dashed triangle) in the bottom of the trough. The symmetric configuration is shown by the solid line.

The nuclear motion in the bottom of the trough for the JT $E \otimes e$ problem is described in ref. 94. The metal sites of a distorted triangle move along the circles so that the phases of sites 2 and 3 are shifted by the angles $2\pi/3$ and $4\pi/3$, respectively, to the phase of site 1. Fig. S8 shows an instant nuclear configuration in course of this motion in which the edge 1-2 is elongated while the edge 1-3 and 2-3 are compressed, taking advantage from the new exchange network. In this geometry of an isosceles two antiferromagnetic pathways 1-3 and 2-3 are energetically favorable while the connection 1-2 is ferromagnetic. One can see that the system possesses a definite spin alignment so that spin frustration is eliminated by the Jahn-Teller distortion with the instant isosceles configuration corresponding to $S_{12} = 1$ in the ground state (Fig. S8). Since the orbital degeneracy is removed the magnetic anisotropy

(caused by the AS exchange) is reduced.[95] More careful analysis shows also that the vibronic interaction proves to be competitive to the AS exchange.

In general, the shape of the surfaces depends on the relation between the AS exchange δ (dimensionless parameter, in the units of the vibrational quantum) and vibronic coupling that proved to be competitive. In the case of weak vibronic coupling and/or strong AS exchange $\upsilon^2 < 4|\delta|/3$ the lower surface possesses a single minimum at $Q_x = Q_y = 0$ so that the symmetric (trigonal) configuration of the system proves to be stable. In the opposite case of strong vibronic interaction and/or weak AS exchange, $\upsilon^2 > 4|\delta|/3$, the symmetric cluster configuration is unstable. In fact, one can see (Fig. S7c) that the maximum symmetry point $Q_x = Q_y = 0$ in the Q space corresponds to the top in lower adiabatic surface. The minima form a ring of the radius ρ_0 at the bottom of the trough:

$$\rho_0 = \tfrac{1}{2}\sqrt{3\upsilon^2/2 - 8\delta^2/3\upsilon^2}\,. \qquad \text{(eq. 6)}$$

The radius ρ_0 decreases with the increase of AS exchange and vanishes at $\delta = 3\upsilon^2/4$. These two types of the pseudo-JT surfaces are shown in Fig. S7b and Fig. S7c. Therefore the AS exchange tends to keep symmetric geometric configuration, thus acting against the JT effects.

Fig. S9 shows a section of the adiabatic potential along the energy axis in the case of JT instability. One can see that in each instant geometrical configuration of the system defined by the coordinate ρ (and arbitrary polar angle φ at the bottom of the 'sombrero'), the zero-field splitting of the ground state $[\delta^2 + (3/2)\,\upsilon^2\rho^2]^2$ is increased with respect to the initial (i.e. in the absence of the JT effect) AS splitting. The maximum splitting is reached when the system runs along the bottom of the 'sombrero'. The eigenstates of the AS exchange Hamiltonian, eq. 2, belong to a definite spin chirality (+ and –) and at the same time can be characterized by the definite values of the so-called 'pseudo-angular' momentum projection $M_L = 1$ or $M_L = -1$ onto the C_3 axis of quantization (see details in refs. 36, 39, and 40). On the contrary, the JT distortions mix the states with a given chirality and create the states with the broken axial symmetry that belong to the definite values of the intermediate spin values and do not possess a definite spin chirality. These situations are illustrated qualitatively by the correlation diagram in Fig. S10. The interrelation between the eigenstates of AS exchange Hamiltonian and JT states so far discussed shows that the vibronic pseudo-JT coupling arising from the modulation of the exchange interaction by the double degenerate molecular vibrations is able to reduce AS exchange and giving rise to a restoration of the magnetization quenched by AS exchange. This leads to an essential reduction of the magnetic anisotropy in

spin-frustrated triangular clusters so that in the limit of strong JT coupling the isotropic exchange model becomes adequate.

The Jahn-Teller effect strongly affects the magnetic properties of the frustrated triangular systems in the crossing/anticrossing region (see Fig. 5) giving rise to an additional effective deformation of the system. Again, the AS exchange and structural deformation of the triangle are competitive.[95]

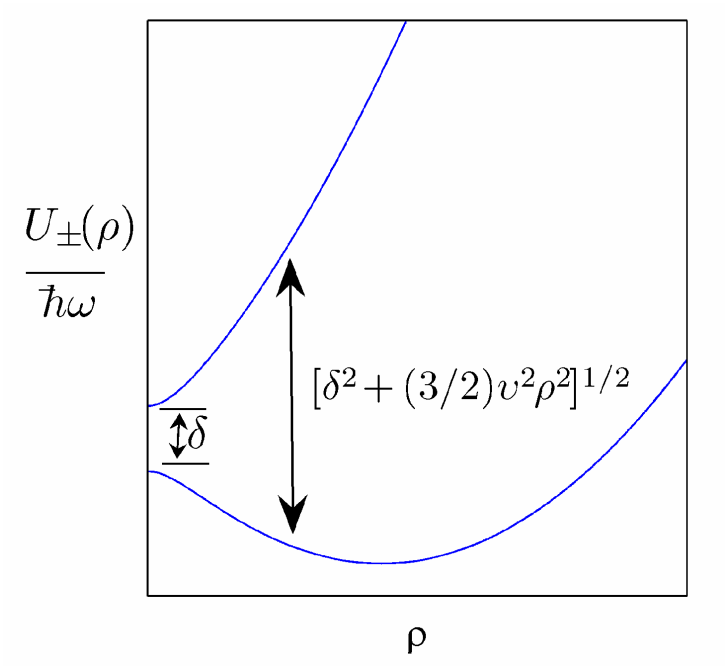

Fig. S9 A section of the adiabatic potentials in the case of JT instability, illustrating the zero-field splitting of the ground state in vibronically distorted configurations (δ = 1, υ = 3.0).

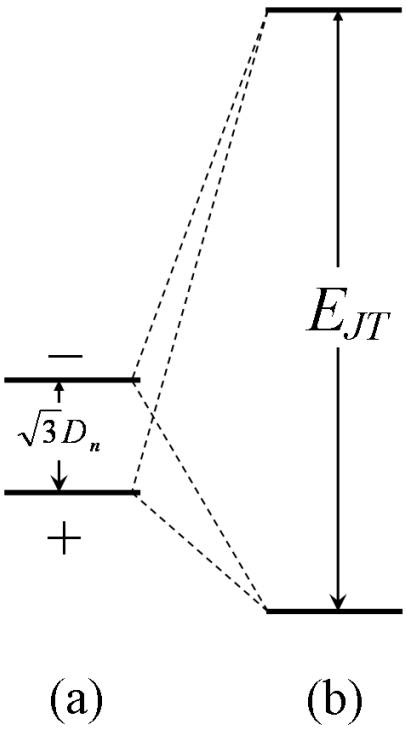

Fig. S10 Correlation of the eigenstates of the AS exchange Hamiltonian and JT states: (a) in the limit of weak JT coupling, the states with their given chirality, (b) in the limit of strong JT coupling.

References

(See main manuscript for references 1-80.)

81. G. Toulouse, *Commun. Phys*., 1977, **2**, 115-119.
82. A. Bencini and D. Gatteschi, *Electron Paramagnetic Resonance of Exchange Coupled Systems*, Springer, Berlin, 1990.
83. K. Matan, D. Grohol, D. G. Nocera, T. Yildirim, A. B. Harris, S. H. Lee, S. E. Nagler and Y. S. Lee, *Phys. Rev. Lett.*, 2006, **96**, 247201/1-4.
84. (*a*) P. W. Anderson, *Science*, 1987, **235**, 1196-1198; (*b*) X. G. Wen, F. Wilczek and A. Zee, *Phys. Rev. B*, 1989, **39**, 11413-11423.
85. M. P. Shores, B. M. Bartlett and D. G. Nocera, *J. Am. Chem. Soc.*, 2005, **127**, 17986-17987.
86. M. P. Shores, E. A. Nytko, B. M. Bartlett and D. G. Nocera, *J. Am. Chem. Soc.*, 2005, **127**, 13462-13463.
87. B. M. Bartlett and D. G. Nocera, *J. Am. Chem. Soc.*, 2005, **127**, 8985-8993.
88. D. Grohol, K. Matan; J.-H. Cho, S.-H. Lee, J. W. Lynn, D. G. Nocera and Y. S. Lee, *Nature Mater.*, 2005, **4**, 323-328.

89. B. M. Bartlett, D. Grohol, D. Papoutsakis, M. P. Shores and D. G. Nocera, *Chem. Eur. J.*, 2004, **10**, 3850-3859.
90. T. Inami, M. Nishiyama, S. Maegawa and Y. Oka, *Phys. Rev. B*, 2000, **61**, 12181-12186.
91. M. Elhajal, B. Canals and C. Lacroix, *Phys. Rev. B*, 2002, **66**, 014422/1-6
92. L. N. Bulaevskii, C. D. Batista, M. V. Mostovoy and D. I. Khomskii, *Phys. Rev. B*, 2008, **78**, 024402.
93. (*a*) R. Schmidt, J. Richter and J. Schnack, *J. Magn. Magn. Mater.*, 2005, **295**, 164-167; (*b*) J. Schnack, *J. Low Temp. Phys.*, 2006, 279-284.
94. (*a*) R. Englman, *The Jahn-Teller Effect in Molecules and Crystals*, Wiley, 1972; (*b*) I. B. Bersuker and V. Z. Polinger, *Vibronic Interactions in Molecules and Crystals*, Springer, Berlin,1989; (*c*) I. B. Bersuker, *The Jahn-Teller Effect*, Cambridge University Press, Cambridge, 2006.
95. (*a*) A. Tarantul, B. Tsukerblat and A. Müller, *Solid State Sci.*, 2008, **10,** 1814-1819; (*b*) A. Tarantul, B. Tsukerblat and A. Müller, *J. Mol. Struct.*, 2008, **890**,170-177.